Ecological Indicators 179 (2025) 114219

Contents lists available at ScienceDirect

Ecological Indicators

journal homepage: www.elsevier.com/locate/ecolind

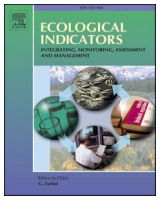

Original Articles

Long-term phenological shifts in coastal saltmarsh vegetation reveal complex responses to climate change

Jing Feng [a,b,*], Tim J. Grandjean [a], Xuerong Wu [a,c], Johan van de Koppel [a,d], Daphne van der Wal [a,b]

[a] NIOZ Royal Netherlands Institute for Sea Research, Dept Estuarine and Delta Systems, P.O. Box 140, 4400 AC Yerseke, the Netherlands
[b] Faculty of Geo-Information Science and Earth Observation (ITC), University of Twente, P.O. Box 217, 7500 AE Enschede, the Netherlands
[c] Department of Physical Geography, Faculty of Geosciences, Utrecht University, P.O. Box 80.115, 3508 TC Utrecht, the Netherlands
[d] Groningen Institute for Evolutionary Life Sciences, University of Groningen, P.O. Box 11103, 9700 CC Groningen, the Netherlands

ARTICLE INFO

Keywords:
Phenology
Climate change
Western Scheldt estuary
Saltmarsh vegetation
Growing season
Landsat
Remote sensing

ABSTRACT

The impacts of climate change on vegetation growth are attracting increasing global attention. While phenological changes have been extensively studied in terrestrial ecosystems, long-term temporal research on phenology-climate feedback in coastal saltmarsh ecosystems, particularly both at the community and species levels, remains limited. In this study, the spatial phenology of saltmarsh vegetation was studied in the Dutch Western Scheldt estuary over three decades (1993–2022), based on the Landsat satellite-derived 2-band enhanced vegetation index (EVI2), coupled to existing sequential maps of vegetation communities. Our results show that saltmarsh vegetation in specific zones greens up earlier, reaches peak greenness sooner, and undergoes a significantly extended growing season—patterns are broadly consistent with climate-driven shifts observed in other ecosystems. However, phenological responses varied across the tidal inundation gradient, with higher intertidal communities initiating growth earlier than lower zones, reflecting the added complexity introduced by future sea-level rise and altered hydrological regimes. Correlations with seasonal meteorological variables showed spatially variable effects: warmer springs advanced green-up, drier summers delayed peak growth and senescence, and higher winter precipitation extends the growing season. Moreover, phenological asynchrony among plant species underscores the influence of species-specific traits and adaptive strategies. Saltmarsh vegetation shows both broad phenological responses to changes in meteorological conditions and site-specific patterns influenced by tidal regimes. Species composition and environmental gradients drive these responses, highlighting the need to understand these interactions for targeting vulnerable species, guiding restoration, and maintaining key ecosystem services (such as carbon sequestration, flood risk reduction, and habitat provision) under climate change.

1. Introduction

Climate change is accelerating at an unprecedented rate, with 1.5 °C warming expected within the next decade (Lee et al., 2021; Forster et al., 2024). Rising temperatures drives increased frequency of extreme events, like heatwaves, droughts, and heavy rainfall (Cardell et al., 2020; Robinson et al., 2021; Vautard et al., 2023), with cascading effects on biodiversity and ecological community structure worldwide (Antão et al., 2020). These changes drive plant phenology shifts—such as earlier spring onset and delayed autumn senescence—although the shifts vary across geographic gradients, climate zones, ecosystems and plant species (Richardson et al., 2013; Chmura et al., 2019; Antala et al., 2022; Meng et al., 2024; Mo et al., 2024). Phenological shifts can directly influence key ecosystem functions—such as biomass production (Peichl et al., 2018), photosynthetic efficiency (Meng, et al., 2023), carbon sequestration (Antala et al., 2022; Ren et al., 2024) and multitrophic species interactions (Morellato et al., 2016). These impacts emerge via altered energy flows, nutrient cycling efficiency, and species dynamics. However, climate-driven phenological mismatches can disrupt these relationships, leading to serious consequences like plant establishment failure and resource scarcity (Morellato et al., 2016; Renner and Zohner, 2018). Thus, phenological shifts can serve as both indicators of

* Corresponding author at: NIOZ Royal Netherlands Institute for Sea Research, Dept Estuarine and Delta Systems, P.O. Box 140, 4400 AC Yerseke, the Netherlands.
E-mail address: jing.feng@nioz.nl (J. Feng).

https://doi.org/10.1016/j.ecolind.2025.114219
Received 6 April 2025; Received in revised form 10 September 2025; Accepted 12 September 2025
Available online 20 September 2025
1470-160X/© 2025 The Author(s). Published by Elsevier Ltd. This is an open access article under the CC BY license (http://creativecommons.org/licenses/by/4.0/).

environmental stress and predictors of ecosystem recovery trajectories (Dronova and Taddeo, 2022). Historical phenological analysis reveals ecosystem sensitivity to climate variability (Richardson et al., 2013; Meng et al., 2024; Mo et al., 2024) while informing critical assessments of carbon storage, habitat dynamics, and broader ecosystem services (Miller et al., 2021; Dronova et al., 2022). Additionally, while temperature is the dominant driver of phenology, other factors such as precipitation, evapotranspiration, water availability, and photoperiod also play critical roles—particularly in modifying thermal thresholds (Fu et al., 2014; Piao et al., 2019a) and determining the temporal distribution of phenophases (Meng et al., 2024).

Despite advances in terrestrial systems, coastal phenology—particularly saltmarsh full seasonal phenological dynamics and their relationships with climatic stressors—have received far less attention (Kromkamp and Van Engeland, 2010; Mo et al., 2015, 2017; Miller et al., 2021). Saltmarshes are dynamic intertidal ecosystems where halophytic plants thrive, providing key services such as carbon storage, biodiversity support, habitat provision, wave attenuation, and shoreline protection (Van de Koppel et al., 2005; Van der Wal et al., 2008; Laengner et al., 2019; Temmerman et al., 2023). Unlike terrestrial ecosystems, saltmarshes experience unique stressors such as tidal inundation and salinity—that are highly sensitive to climate warming, particularly through sea-level rise—which may lead to distinct phenological responses (Chen and Kirwan, 2022; Zhang et al., 2024). Specifically, tidal forcing can reshape the zonal distribution of saltmarsh plants by altering flooding frequency, soil permeability, and soil chemistry—including the enrichment of plant-growth-related compounds like CO_2 (Wang et al., 2024). Furthermore, the energy expended on salt regulation reduces resources available for growth and reproduction, ultimately altering key plant life-cycle stages, such as germination and growth rate (Gallego-Tévar et al., 2019). By intensifying flooding and salinity stress, sea-level rise compels saltmarshes to adapt via landward migration or vertical sediment accretion, leading to phenological shifts such as a compressed growing season and altered reproductive timing (Mo et al., 2019). In addition, saltmarshes, like terrestrial ecosystems, comprise multiple plant species whose phenological responses to climate change may differ (Shen et al., 2019). These species-specific sensitivities can interact to shape the overall ecosystem response, where asynchronous growth dynamics may enhance ecosystem stability under interannual climate variability—an effect previously observed in terrestrial systems (Stevens and Carson, 2001; Dronova and Taddeo, 2022). Understanding how saltmarsh plant species have responded to recent climatic variations can thus provide insights into future resilience and inform adaptive coastal management strategies (Morellato et al., 2016; Mo et al., 2017; Buffington et al., 2018).

It's necessary to address prior limitations in spatiotemporal scope, methodological simplicity and vegetation composition analysis for filling a critical gap in coastal ecosystem research. In particular, satellite data (e.g., Landsat) enable landscape-scale monitoring, overcoming field-based limitations (Dronova and Taddeo, 2022). Therefore, this study employs advanced phenological extraction techniques (Kong et al., 2022) to investigate the long-term impacts of climate change on saltmarsh vegetation phenology, with a focus on the Dutch Western Scheldt estuary (1993–2022). We focus on spatial phenological shifts, their climate drivers, and species-specific responses. We hypothesize that coastal phenology follows warming trends similar to terrestrial systems, but with modulation by tidal emergence gradients. Additionally, we propose that species-specific responses in saltmarshes reflect trade-offs between meteorological and inundation stressors. Here, the following scientific questions are addressed: 1) How has the phenology of saltmarsh vegetation changed over time? 2) How are these phenological changes influenced by the tidal emergence gradient characteristic of coastal saltmarshes? 3) How does historical climatic change relate to the phenological dynamics of saltmarsh vegetation? To this end, we quantitatively assess changing patterns in the phenological metrics of saltmarsh vegetation in the Western Scheldt estuary and their responses to key climate factors.

2. Material and methods

2.1. Research area

The Western Scheldt, a tide-dominated estuary in southwest Netherlands flowing into the North Sea, features a longitudinal salinity gradient, numerous tidal flats, hosting diverse habitats for birds, fish, and saltmarsh vegetation (Tavora et al., 2023), including Saeftinghe, Europe's largest saltmarsh area (Fig. 1). The Western Scheldt connects the seaports of Vlissingen and Terneuzen (Netherlands); it borders the upper estuarine Sea Scheldt in Belgium with the ports of Antwerp and Ghent (Belgium) (Meire et al., 2005). The salinity gradient in the Dutch part of the estuary ranges from near-marine salinity near the mouth to brackish waters upstream. Mean annual river discharge from the rain-fed Scheldt is between 100 and 200 m^3s^{-1} (Meire et al., 2005); river discharge is low in summer (on average 60 m^3s^{-1}) and higher in winter (on average 180 m^3s^{-1}) (Baeyens et al., 1998). During spring tides, the tidal range is 4.45 m near the mouth and 5.67 m in the brackish section of the Western Scheldt close to the Dutch-Belgium border (Rijkswaterstaat, 2016). In such macrotidal systems, saltmarsh dynamics are predominantly governed by tidal processes, sustaining high salinity levels within the marsh environment (Yando et al., 2023). In our downstream estuarine study area (brackish to saline zone), elevation dominates over salinity in structuring saltmarsh plant zonation within the tidal gradient (Feng et al., 2025). The Western Scheldt estuary features a temperate climate with predominantly southwesterly winds, cool summers, mild winters, and around 900 mm of evenly distributed annual precipitation (De Vriend et al., 2011). Based on the Royal Netherlands Meteorological Institute (KNMI) data from the Vlissingen monitoring station (1993–2022), the mean annual temperature was 11.3 $\pm$ 0.7 °C, with average monthly extremes of 14.1 $\pm$ 5.9 °C (maximum) and 8.8 $\pm$ 4.9 °C (minimum). Over recent decades, an overall increase in annual average temperature has been observed (Kromkamp and Van Engeland, 2010). The typical pioneer plant species are the perennial cord grass (*Spartina anglica*) and the annual glasswort (*Salicornia* spp.). In the upper marsh, vegetation composition becomes more diverse, including species such as common saltmarsh grass (*Puccinellia maritima*), annual seablite (*Suaeda maritima*), sea aster (*Aster tripolium*), seaside bulrush (*Bolboschoenus maritimus*), and common reed (*Phragmites australis*) (Van der Wal et al., 2008).

2.2. Methods

2.2.1. Meteorological data

We used seasonal meteorological variations as a proxy for local climate change, focusing on four key factors: temperature, precipitation, drought conditions, and sunshine duration. Data (1993–2022) for the monthly average temperatures, amount of precipitation and sunshine duration were used from KNMI station Vlissingen (Fig. 1a). We chose a drought index, the Standardized Precipitation-Evapotranspiration Index (SPEI), which integrates precipitation and temperature-driven evapotranspiration, providing an effective measure of the cumulative water balance between atmospheric supply and demand (Beguería et al., 2014). The Global SPEI database, SPEIbase, with monthly data with a 0.5 degrees spatial resolution was used in this research. We selected for this study the pixel (51.25°, 3.75°), which is the nearest by the Western Scheldt estuary. The study involved the indexes "SPEI_3", which represents a standardized index quantifying how a 3-month accumulated surface water balance (precipitation minus potential evapotranspiration) deviates from its expected value for that period (Vicente-Serrano et al., 2010). The positive values present wet conditions while negative values present dry conditions. To better understand the relationship between phenological events of vegetation growth and climate change, we recalculated the climatic data of each season for each year. Given the

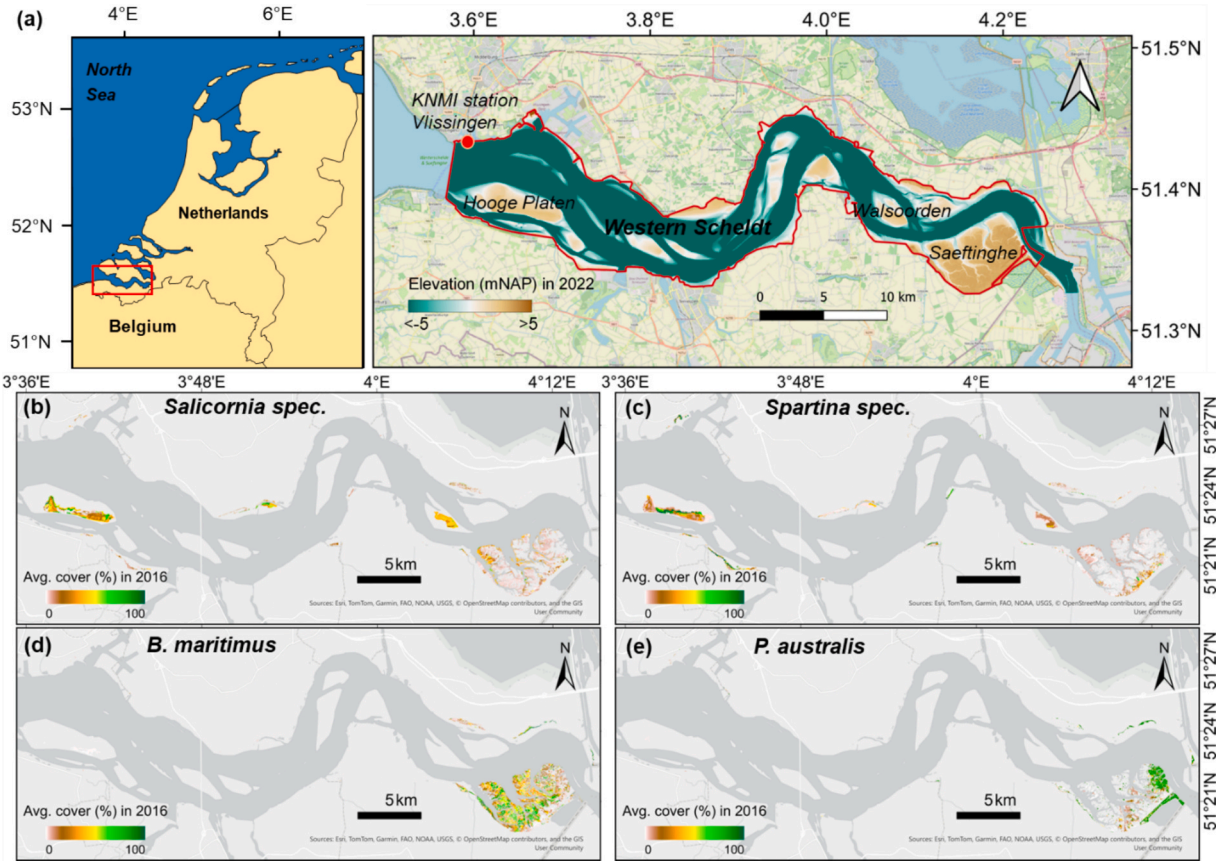

Fig. 1. (a) Location of the Western Scheldt estuary (southwest Netherlands); (b-e) the distribution of four dominant vegetation species in 2016. Note. (a) The red boundary on the right of the subfigure shows the 2016 embanked area. Elevation data (2022) were obtained from Rijkswaterstaat (Methods 2.2.2). (b-e) Vegetation data are derived from Rijkswaterstaat's 2016 vegetation map (Methods 2.2.2). All backgrounds of geographical maps were generated using ArcGIS Pro (ESRI, 2023). (For interpretation of the references to colour in this figure legend, the reader is referred to the web version of this article.)

lagged effects of climate factors on vegetation growth, winter refers to three months from December the last year to February in the recent year. Spring spans the time period from March to May. Summer includes the time from June to August. September, October and November are classified as Autumn. Based on these seasons, we can calculate the corresponding seasonal data of climatic factors.

2.2.2. *Changing patterns in vegetation phenology*

We selected a 2-band enhanced vegetation index (EVI2) (Jiang et al., 2008) time series to extract and process the vegetation phenology with remote sensing. Unlike NDVI, EVI2 is better at identifying diverse land cover and timing the greening season due to its reduced saturation in dense vegetation (Sun et al., 2023). Therefore, we firstly collected the time-series EVI2 for each year from the observations of satellites (Landsat 5, 7, 8, see Table S1) during the past three decades (1993–2022) using Google Earth engine (GEE) (Gorelick et al., 2017). The images of Landsat 7 after 31 May 2003 were excluded due to the failure of the scan line corrector. Here, the surface reflectance of the near-infrared (NIR) and red bands by the Landsat images were used to calculate EVI2:

$$EVI2 = 2.5 \bullet \frac{\rho_{NIR} - \rho_{Red}}{\rho_{NIR} + 2.4 \bullet \rho_{Red} + 1}$$

where ρ_{NIR} and ρ_{Red} are the surface reflectance of the near-infrared band and red band of the Landsat image, respectively. To reach a good balance of fidelity and smoothness, we applied a robust denoising approach (weighted Whittaker (Eilers, 2003; Kong et al., 2019)) to reconstruct remote sensing vegetation indices and extracted pixelwise annual phenological metrics using the derivative method (Filippa et al., 2016; Zhang et al., 2018; Kong et al., 2020) with the R package *phenofit* (Kong et al., 2022). The detailed metrics include the start/end/peak/length of the growing season (respectively, SOS/EOS/POS/LOS, see Fig. 2). Specifically, the derivative method calculates the first-order derivative of the vegetation time series, where SOS and EOS are defined as the day of maximum growth rate and senescence rate, respectively, and POS is the peak value in the original time series (Kong et al., 2022). Additionally, LOS is derived as the temporal difference between EOS and SOS. The

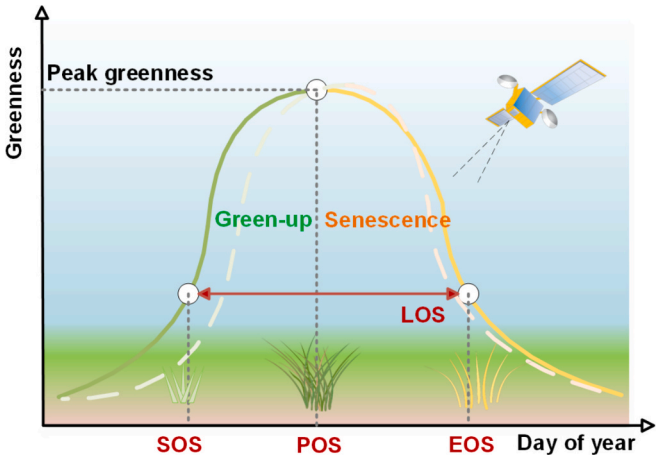

Fig. 2. Conceptual diagram of key parameters concerning remote sensed vegetation phenology. Note. SOS/POS/EOS/LOS represents the Start/Peak/End/Length of vegetation growing Season.

Theil-Sen estimator was employed to analyze pixel-wise temporal trends in the phenological parameters (SOS, POS, EOS and LOS) over the past three decades (Sen, 1968). Additionally, the Mann-Kendall test was applied to the entire time series to determine the significance of these trends at each pixel (Mann, 1945). In our study, to minimize tidal change effects and reduce the impact of abrupt land-use changes, thereby ensuring more representative long-term phenological data, we selected pixels that were classified as saltmarsh (vegetated status) for at least half the study period (≥15 years), with valid phenological metrics (non-NA values) for at least one-third of the time (≥10 years), as indicated by our sensitivity analysis (See Table S2 and S3). To define the saltmarsh extent for each year, we used ecotope maps (1996, 2001, 2004, 2008, 2010, 2011, 2012, 2015, 2016, 2018, 2020, 2022) and vegetation maps (1993, 1998), available from the Ministry of Infrastructure and Water Management of the Netherlands—Rijkswaterstaat (https://rijkswaterstaatdata.nl/). Rijkswaterstaat regularly classifies the Western Scheldt into ecotopes—distinct ecomorphological units—based on criteria such as elevation, depth, flow velocity, inundation duration, salinity, and sediment composition. Vegetation maps from 1993 (Von Asmuth et al., 1996), 1998 (Koppejan, 2000), 2004 (Reitsma, 2006), 2010 (Pranger and Tolman, 2012), and 2016 (Reitsma and de Jong, 2018), derived from Rijkswaterstaat, were created by manually delineating homogeneous areas as vector polygons from 1:5000 or 1:10000 aerial photographs, supported by field surveys conducted at plot sites. All above data were used to map the saltmarsh extent in each year. Satellite remote sensing images can estimate extents for unmapped years, provided there are sufficient cloud-free, low tide observations (Laengner et al., 2019; Laengner and Van der Wal, 2022), albeit with a lower spatial resolution. Our analysis relied exclusively on existing ecotope and vegetation maps based on aerial photographs for saltmarsh delineation. The intersecting saltmarsh boundaries from the nearest two mapped years were used to estimate extent for unmapped years (Fig.S1). Meanwhile, spatial distributions of averaged phenological metrics were also detected. To clarify phenological distribution trends, emersion duration and elevation maps (1996, 2001, 2004, 2008, 2010, 2011, 2012, 2015, 2016, 2018, 2020, 2022) with a 20 m × 20 m resolution from Rijkswaterstaat were also utilized. The elevation dataset was generated by integrating airborne LIDAR topography with shipborne multibeam and single-beam bathymetry, both standardized to meters relative to NAP (the Dutch ordnance datum). Furthermore, emersion duration maps were derived from 20 m × 20 m elevation data and water level measurements relative to m NAP. The water level data, recorded every 10 min by Rijkswaterstaat at five tide gauge stations along the Western Scheldt, covered the preceding three years. Emersion duration was calculated based on the dominant M2 tidal component (Kers et al., 2013). We applied reduced major axis regression (Harper, 2016) to examine correlations between average phenological metrics and both average elevation and emersion duration respectively.

2.2.3. The response of vegetation phenology to climate change

Spatially, the Pearson correlation method and Bonferroni correction were used to analyze the correlations between average vegetation phenology and environmental drivers for each pixel. To account for temporal variations and mitigate potential multicollinearity among climatic variables, partial correlation analysis (Legendre, 2000; Meng, et al., 2023; Bao et al., 2024; Xu et al., 2024) was employed to examine the seasonal effects of each primary climatic factor on vegetation phenology, controlling for the influence of other variables over the past three decades. The partial correlation analysis involved 16 climatic drivers consisting of four seasons of temperature, precipitation, drought index (i.e. SPEI) and sunshine duration over past 30 years. The dominant factor for each phenological metric is identified as the variable that has the highest number of pixels with significant partial correlation coefficients, after accounting for the influence of other variables. As for the LOS, we listed top four dominant climatic factors considering similar amount. To better compare responding differences among different plant species, vegetation distribution maps from 1993 (Von Asmuth et al., 1996), 1998 (Koppejan, 2000), 2004 (Reitsma, 2006), 2010 (Pranger and Tolman, 2012), and 2016 (Reitsma and de Jong, 2018) were used to illuminate the sensitivities of abundant plant species phenology to climate change. The four most abundant plant species were determined by their total cover across all five sequential vegetation maps (Feng et al., 2025). These include the annual species: (1) *Salicornia spec.* (specifically *Salicornia europaea* and *Salicornia procumbens*), and the perennial species: (2) *Spartina spec.* (including *Spartina anglica* and *Spartina townsendii*), (3) *Bolboschoenus maritimus*, and (4) *Phragmites australis* (Fig. 1b–e). Based on the vegetation maps, we selected the pixels meeting the following conditions to represent each individual abundant plant species: (1) total cover in a certain year is greater than 50 %; (2) the proportion of a certain plant species is greater than 50 %. We assumed the above selected pixels are vegetated and dominated by certain plant species. To assess how vegetation composition influences phenological shifts, we analyzed the four most abundant species from the latest available vegetation map (2016). For each vegetated pixel, we designated the species with highest coverage as dominant to assess composition-related phenological changes. We then adding the density plots demonstrating the distribution of different vegetation communities across the tidal emergence gradient. Furthermore, we added pie charts showing area proportions of pixels with dominant trends, highlighting significant positive or negative slopes or correlations in each map. All relevant spatial and statistical analyses were implemented in ArcGIS Pro (ESRI, 2023) and R v.4.3.2 (R Core Team, 2023).

3. Results

3.1. Changes in saltmarsh vegetation phenology

Most saltmarshes in our study showed no significant phenological changes. However, pixels with significant change were spatially clustered: in some areas, we observed an earlier onset and an earlier peak of the season, causing an extended growing season as time progressed (Fig. 3). Specifically, spring phenology shifted significantly in 11.75 % of the saltmarsh areas, with most regions—particularly in Saeftinghe, intertidal shoals, and some coastal zones—showing earlier onset (Fig. 3a). An exception to this trend was observed at some of the higher elevations within Saeftinghe, where SOS occurred later (Fig. 3a). Similar changing patterns of POS were also detected at these elevated locations (Fig. 3b). The timing of vegetation senescence varied spatially, with significantly delayed EOS primarily occurring in the eastern high-lying zones of Saeftinghe, while advanced EOS was detected in some other parts of the saltmarsh (e.g. in Zuidgors and some areas of Saeftinghe, EOS seemed mostly earlier, not later) (Fig. 3c). The significantly extended LOS were prevalent across most intertidal areas including Saeftinghe, Walsoorden and Hooge Platen (Fig. 1 and Fig. 3d). In terms of vegetation succession, communities dominated by *B. maritimus* are associated with earlier SOS and POS, contributing to a longer growing season. Meanwhile, delayed EOS is notably linked to the expansion of *P. australis* (see pie charts in Fig. 3). Additionally, although significant phenological changes were detected only in limited areas, these findings remain ecologically meaningful given the high heterogeneity of the system—particularly for high marsh vegetation communities (Fig.S3), which are more sensitive to meteorological dynamics than to hydrological variations. Specifically, pixels with a significantly earlier SOS accounted for 12.03 % of *Salicornia spec.* (SalSp)-, 15.20 % of *Spartina spec.* (SpaSp)-, 10.72 % of *B. maritimus* (BolMa)-, and 3.88 % of *P. australis* (PhrAu)-dominated communities; pixels with a significantly earlier POS represented 10.67 % of SalSp-, 15.33 % of SpaSp-, and 7.94 % of PhrAu-dominated communities; pixels with a significantly delayed EOS comprised 11.16 % of PhrAu-dominated communities; pixels with a significantly longer LOS covered 15.26 % of BolMa- and 16.47 % of PhrAu-dominated communities (Table S4).

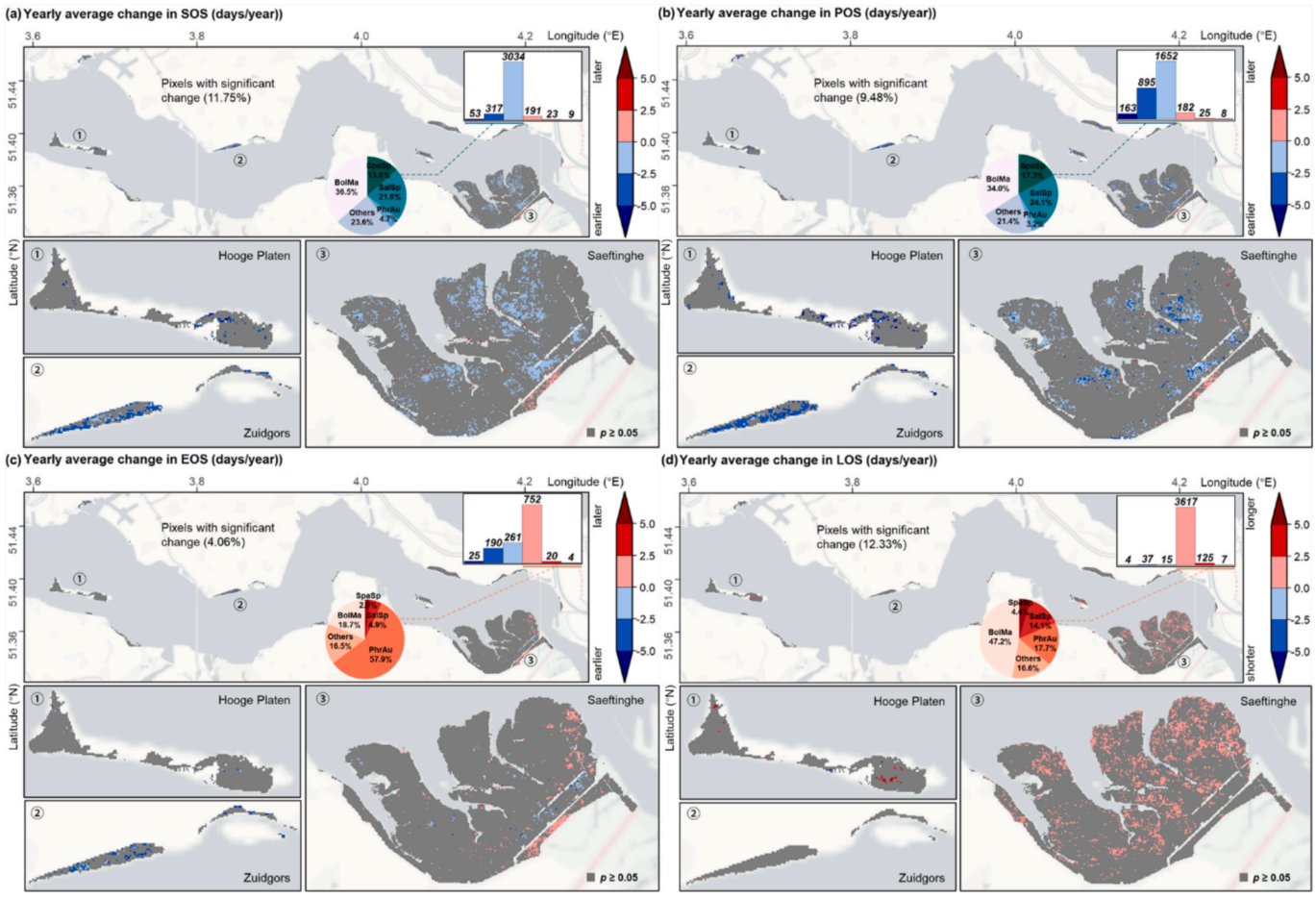

Fig. 3. Spatial distribution of the temporal trend in phenological metrics ((a) SOS; (b) POS; (c) EOS; (d) LOS) in the saltmarshes of the Western Scheldt. Note. Spatial patterns of long-term average phenological metrics can be found in Fig. S2. The histogram on the top of each map shows the quantity distribution of the pixels with significant change ($p < 0.05$). The colors of bars in each histogram are consistent with the ones of each map legend. Grey filled pixels indicate non-significant changing trend ($p \geq 0.05$). The red pie chart corresponds to the red section of the histogram (delay in the season or longer growing season), while the greenish pie chart corresponds to the blue section of the histogram (earlier in the year or shorter growing season). SpaSp means *Spartina spec.*, SalSp means *Salicornia spec.*, BolMa means *B. maritimus* and PhrAu means *P. australis* in the pie chart. See also Table S4 and Fig. S3 for complementary information of the pie charts. (For interpretation of the references to colour in this figure legend, the reader is referred to the web version of this article.)

3.2. Vegetation phenology patterns across the tidal emergence gradient

We observed weak, negative relationships between SOS, POS, EOS, and emersion time. Vegetation growth in higher intertidal zones with greater tidal emergence generally began and peaked earlier than in the mid and lower intertidal zone (Fig. 4 and Fig. S4). With increasing elevation, the growing season length tends to extend (Fig. S4d). We found that *B. maritimus* and *P. australis* dominated the high-lying areas (top density plots in Fig. 4).

3.3. Meteorological drivers of vegetation phenology

Overall, no significant correlations were found between the timing of phenological events and seasonal average water availability or temperature in saltmarshes after applying the Bonferroni correction (Fig. S6). However, spatially, spring temperatures are significantly linked to green-up in 8.61 % of the saltmarsh, with most areas showing a correlation between warmer springs and an earlier SOS (Fig. 5a). Spring water availability or drought conditions (SPEI) significantly impact the timing of the growing season peak (POS) in 9.07 % of the saltmarsh, with most areas showing wetter springs associated with a delayed POS (Fig. 5b). Summer water availability significantly influences the EOS timing in 12.37 % of the saltmarsh, with most areas exhibiting a negative partial correlation, indicating that wetter summers delay the EOS (Fig. 5c). Winter precipitation is the main seasonal factor influencing growing season length, with 16.85 % of saltmarsh areas showing a significant correlation, most exhibiting a positive link between higher winter precipitation and longer growing seasons (Fig. 5d). In terms of vegetation composition, *B. maritimus* is the dominant species, indicating that vegetation communities led by *B. maritimus* are sensitive to variations in spring temperature, summer water availability, and winter precipitation. Additionally, vegetation communities dominated by *P. australis* respond to increased winter precipitation, contributing to an extended growing season (Fig. 5). In particular, four abundant saltmarsh plant species exhibit asynchronous phenological characteristics. The engineer species *Salicornia spec.* exhibits later green-up and senescence, whereas *B. maritimus* is featured as earlier occurrence of SOS and POS; *Spartina spec.* has the shortest growing season due to its early senescence, while *Salicornia spec.* and *B. maritimus* exhibit the longest growing seasons (Fig. 6 and Fig. S8).

4. Discussion

In this study, we demonstrated the phenological dynamics of saltmarsh vegetation marked by spatial variations. First, our case study reveals an earlier onset of greening and a longer growing season in part of the saltmarshes in the Western Scheldt. This tendency aligns with global observed seasonal phenology changes (Piao et al., 2019b; Meng

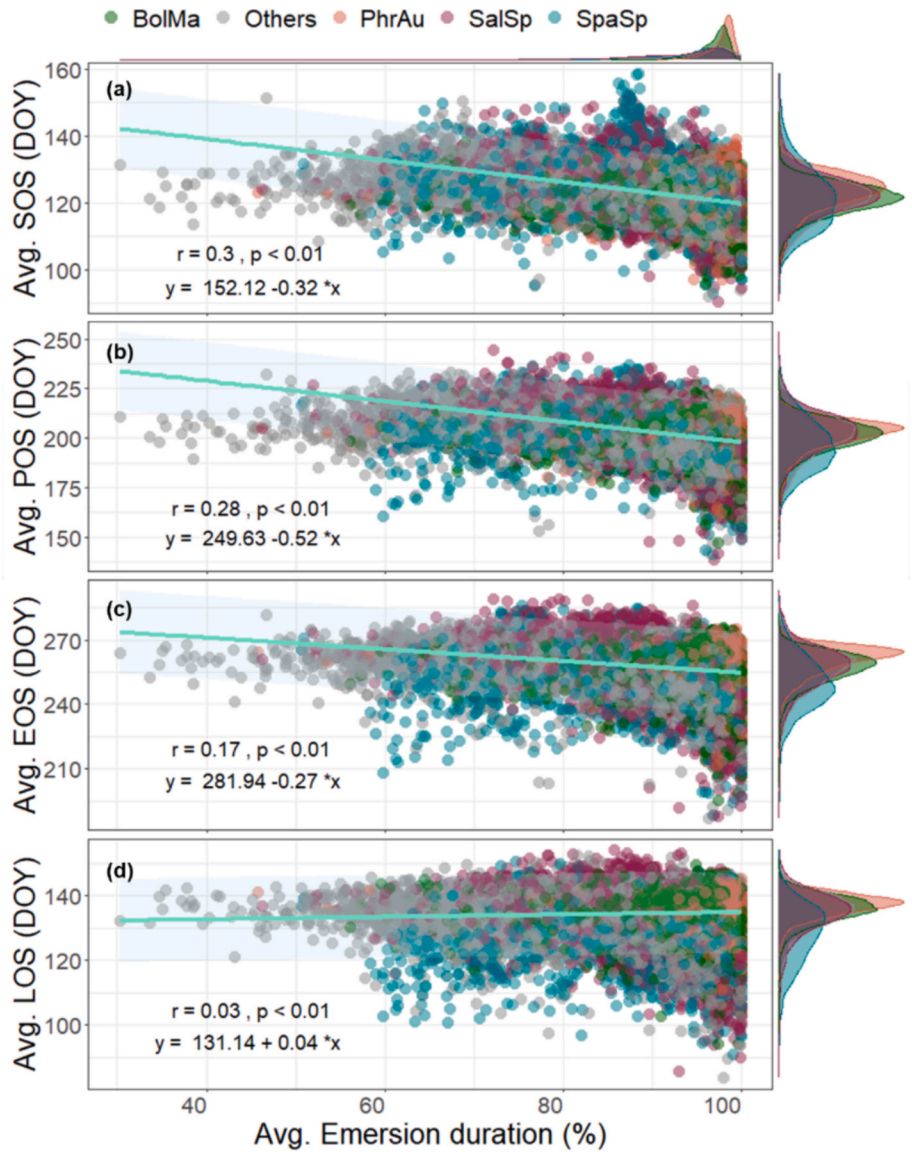

Fig. 4. Relationships between key phenological metrics and emersion duration gradients: (a) SOS; (b) POS; (c) EOS; (d) LOS. Note. Using the 2016 vegetation map, we identified the species with the maximum cover among the four dominant species to classify vegetation community types and analyze their contributions to the distribution of phenological characteristics (See methods 2.2.3). SpaSp means Spartina spec., SalSp means Salicornia spec., BolMa means B. maritimus and PhrAu means P. australis. The symbol r denotes the Pearson correlation coefficient calculated using reduced major axis regression. Species-specific regression results are presented in Fig. S5.

et al., 2024), documented widely in mid- to high-latitude terrestrial ecosystems of the Northern Hemisphere (Jeong et al., 2011; Jiang et al., 2023), as well for saltmarsh-specific phenological patterns (Buffington et al., 2018; Mo et al., 2019), and phytoplankton responses in marine ecosystems (Kromkamp and Van Engeland, 2010). This consistent phenological change may reflect a broad coherence in vegetation response to climate change. However, saltmarshes, as unique ecosystems shaped by tidal inundation, exhibit distinct species compositions and less clear phenological patterns. The interaction between tidal dynamics and local environmental conditions contributes to considerable spatial variability in vegetation distribution (Feng et al., 2025). Following our prior research (Feng et al., 2025), four key species dominate distinct zones along the elevation or emersion duration gradient: *Salicornia spec.*, *Spartina spec.*, *B. maritimus*, and *P. australis*. We found that communities in elevated intertidal areas green up earlier than those in lower or mid elevated zones (Fig. S4), likely due to the distribution of species along the tidal emergence and salinity gradients, where the onset and peak of some pioneer, low and mid marsh species (e.g., *Salicornia spec.*) lag behind those of high marsh species (e.g., *B. maritimus* and *P. australis*) (Fig. 6). As sea-level rise alters inundation regimes, it may further complicate the phenological responses of saltmarsh vegetation to climate change, introducing additional variability and uncertainty. Our findings highlight the importance of incorporating inundation-dependent phenological responses into the planning and management of coastal ecosystem and climate adaptation strategies.

Our results show that seasonal meteorological variation partially influences the phenological patterns of saltmarsh vegetation. In general, spring warming is known to advance leaf unfolding (Piao et al., 2015; Fu et al., 2020), while summer soil moisture deficits can delay peak growth or trigger early senescence, depending on species and regions (Park et al., 2019; Lian et al., 2020). Additionally, winter precipitation may modulate thermal requirements for spring green-up (Fu et al., 2014). Warmer temperatures enhance respiration and photosynthesis, potentially increasing biomass production. For example, spring warming is closely linked to spring leaf onset, as plants in cold and temperate regions typically require a specific accumulation of heat to initiate this

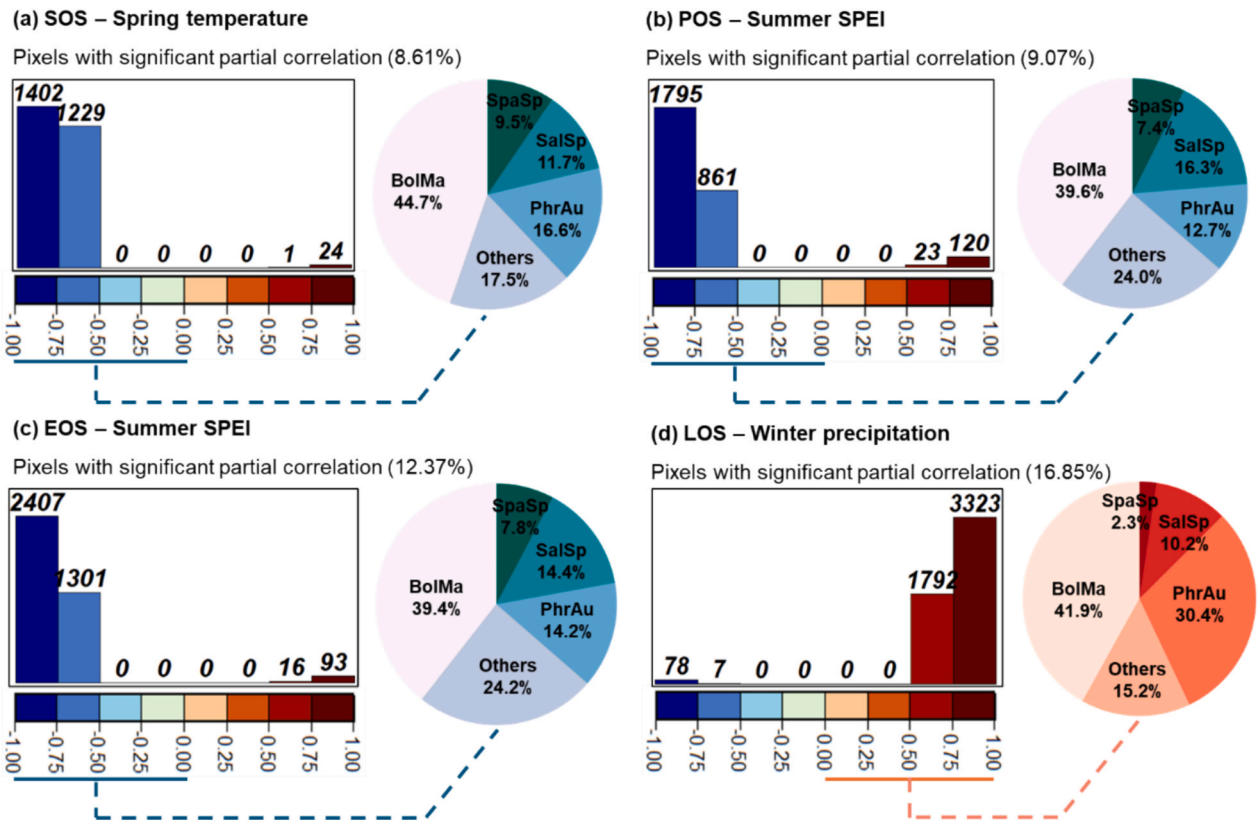

Fig. 5. Dominant meteorological factors influencing the trends of each phenological metric, along with the corresponding vegetation composition for pixels showing significant correlations in each partial correlation. Note: the histograms show the pixels with significant partial correlation coefficient ($p < 0.05$). The red shows significantly positive partial correlations while the blue shows significantly negative correlations in histogram. The distribution of partial correlation coefficients are as follows (a) the effect of spring temperature on SOS, (b) the effect of summer SPEI on POS, (c) the effect of summer SPEI on EOS, (d) the effect of winter precipitation on LOS. The reddish pie chart corresponds to the red section of the histogram, while the greenish pie chart corresponds to the blue section of the histogram. SpaSp means *Spartina spec.*, SalSp means *Salicornia spec.*, BolMa means *B. maritimus* and PhrAu means *P. australis* in the pie chart. The detailed distribution maps of partial correlation coefficients are included in the Appendix (see Fig. S7). (For interpretation of the references to colour in this figure legend, the reader is referred to the web version of this article.)

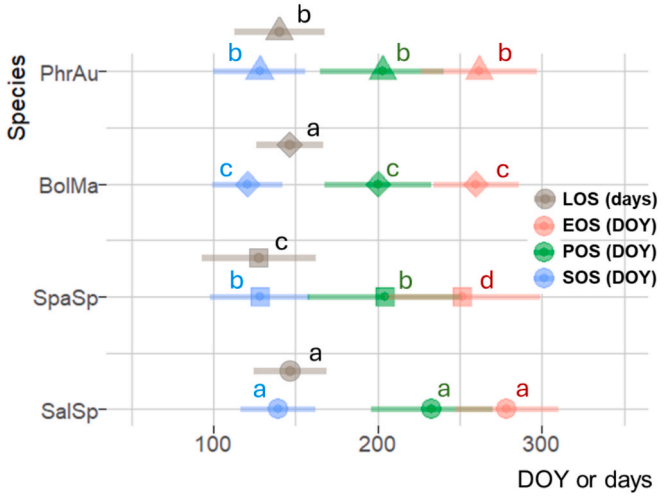

Fig. 6. Phenological metrics of the four abundant plant species, i.e. *Spartina spec.* (SpaSp), *Salicornia spec.* (SalSp), *B. maritimus* (BolMa) and *P. australis* (PhrAu). Different colors represent various phenological metrics, showing averages (symbol) and standard errors (lines). Each set of lowercase letters of the same color denotes significant differences in the corresponding metric with the same color among the four abundant plant species, based on Tukey's HSD and compact letter display, at a 95 % confidence level ($p < 0.05$). Matching letters denote no significant difference in a phenological metric between species, while different letters indicate a significant difference. See also the boxplots in Fig. S8.

process (Piao et al., 2015). However, in salt marshes, warming also elevates porewater salinity through evapotranspiration (Buffington et al., 2018), thereby inducing osmotic stress and impairing water uptake (Flowers and Colmer, 2015). These interactions can alter redox-active biogeochemical processes (Noyce et al., 2023) and vegetation zonation shifts through differential species tolerance (Moffett et al., 2010). The spatial variability in phenological responses likely reflects key plant functional traits, particularly adaptations to flooding regimes and salinity gradients (Mo et al., 2015, 2019). Traits such as root aeration, leaf area, plant height, and salinity tolerance define how plants interact with their environment (Pérez-Harguindeguy et al., 2013). These interactions shape species-specific phenological patterns by influencing sensitivity and resilience (Cleland and Wolkovich, 2024). For instance, shallow rooting can mitigate root hypoxia under waterlogged conditions (Davy et al., 2001), while a low specific leaf area enhances stress tolerance and supports prolonged growth in resource-poor environments (Knight and Ackerly, 2003), as seen in *Salicornia* species. In contrast, deep-rooted species may exhibit delayed flowering and greater drought resilience (Berrached et al., 2017). Such trait-based trade-offs align with distinct ecological strategies—competitive, stress-tolerant, or ruderal (Grime, 1977)—which underlie the timing and duration of phenophases across gradients (Cleland and Wolkovich, 2024). Competitive species such as *P. australis* are tall and form dense stands with well-developed root aeration (Packer et al., 2017), allowing them to capitalize on both early season growth and a prolonged growing period. In contrast, stress-tolerant species like *Salicornia* are short and accumulate salt (Davy et al., 2001), showing delayed green-up and

flexible growth periods. Opportunistic species—particularly the invasive *Spartina*—exhibit rapid early growth but have a shorter growing season.

Our study showed mostly weak or non-significant correlations between phenology and meteorological variables, highlighting the spatial heterogeneity and complexity of these relationships. The few significant partial correlations mainly were detected on the eastern part of the estuary, especially in the saltmarsh of Saeftinghe. Contradictory findings—such as opposite correlations between LOS and winter precipitation (Fig. S7d) versus LOS and winter SPEI (Fig. S7f)—illustrate the nonlinear and multidimensional nature of climate-phenology interactions (Piao et al., 2019b). These discrepancies may have been affected by spatial autocorrelation and covarying factors, which can bias phenology-meteorology relationships. Specially, the relationship between water and temperature is not straightforward. Temperature, radiation, and water may act as co-limiting factors, imposing region-specific constraints on vegetation activity, while temperature-precipitation interactions drive complex, non-linear growth responses across temporal and spatial scales (Dieleman et al., 2012; Wu et al., 2015).

In saltmarshes, precipitation and drought conditions can directly affect soil salinity and waterlogging, thereby influencing plant stress, survival, and biomass production (Buffington et al., 2018). Elevated areas are particularly vulnerable, as salinity varies significantly with elevation. Consequently, rainwater significantly impacts the groundwater and root zone dynamics of more elevated, thus less inundated areas. Building on this, it is vital to note that different responses are also related to distinct growth requirements, such as freshwater availability and photoperiod, at species level (Zeng et al., 2024). More importantly, considering the complex mechanisms or uncertainties in saltmarshes, the oversimplified indicator selection could overlook some essential ecological processes. For example, preseason warming can affect SOS through two competing mechanisms: (1) accelerated heat accumulation promotes earlier SOS, while (2) reduced winter chilling increases thermal requirements, potentially delaying it (Wang et al., 2022). In saltmarshes, however, winter inundation may contra-act this relationship, with water temperature superseding air temperature as the dominant phenological driver. Nevertheless, we recommend future studies incorporate these interacting factors with improved indicator selection.

Saltmarsh plant specific sensitivities to environmental stress play a key role in reshaping vegetation phenological patterns, as evidenced by phenological asynchrony among four dominant species. In high and middle marsh communities, climatic sensitivities of the halophyte *B. maritimus* contribute to an extended growing season with earlier green-up, while *P. australis* exhibits delayed growth onset primarily regulated by humidity and soil nutrient variations (Cleland et al., 2006; Sun et al., 2023). The observed differences may arise from distinct ecological strategies—*B. maritimus* exemplifies a stress-tolerant strategist through its anaerobic adaptations to waterlogged soils (Hroudová et al., 2014), whereas *P. australis* developed as a competitive specialist optimized for stable, less saline, and nutrient-rich habitats (Eller et al., 2017). In low marsh communities, the pioneer species *Salicornia spec.* reaches peak growth in early-to-mid summer, driven by temperature and precipitation. Its spatial distribution controlled by elevation-dependent tidal exposure duration and proximity to nutrient-rich tidal channels (Fivash et al., 2023), while its temporal growth dynamics reflect synergistic regulation by tidal inundation (e.g. via flood/salt-tolerant adaptations) and meteorological factors (Zhu et al., 2019). Drought frequency and severity are also reported to significantly affect its growth (O'Donnell and Schalles, 2016). This is particularly relevant given the cascading effects of changing water content and inundation patterns on the seed productivity of saltmarsh plant species (Zhao et al., 2023). These findings suggest that saltmarsh resilience is governed by species-specific phenological responses to climatic stressors, with distinct tolerance ranges shaping spatial heterogeneity in climate sensitivity. This knowledge can inform predictions of future vegetation dynamics and support adaptive management strategies in coastal ecosystems.

The mechanistic understanding of salt marsh responses to climate change can provide hierarchical and targeted conservation strategies. For example, at the species level, to maintain the biodiversity and counteract climate change impacts on plant-pollinator synchrony, we can plant climate-adapted genotypes (e.g., delayed flowering ecotypes) and design engineering microhabitats (e.g., creating topographic variation to buffer temperature extremes (Suggitt et al., 2018)) in some hotspots or restoration sites. At the habitat scale, by identifying vulnerable species and regions through long-term phenological trends, managers can prioritize habitats critical for ecosystem services. For instance, preserving vegetation patches during critical phenophases safeguards essential stopover forage opportunities for migratory bird populations (Zou et al., 2016). Furthermore, adaptive measures based on the phenological patterns of vegetation communities can enhance primary productivity and carbon sequestration (Mo et al., 2019). Consequently, phenological indices demonstrate strong potential for integration into environmental assessment frameworks, like Wetland Mitigation Banking and blue carbon certification schemes, given their capacity to quantitatively evaluate the functional resilience of ecosystems (Morellato et al., 2016). This approach—spanning species traits, habitat management, and policy frameworks—operationalizes phenological insights for climate-adaptive governance.

Remote sensing overcomes critical limitations of field-based salt marsh monitoring by enabling continuous observation despite recurring tidal influences that disrupt ground surveys. While satellite-derived indicators efficiently track phenological patterns across scales, challenges remain in quantifying interannual variability due to limitations including cloud contamination, sensor resolution constraints, and environmental noise (Piao et al., 2019b). This case study assumes uniformity among the three sensors (Landsat 5, 7, and 8), disregarding their inherent differences. However, tidal marsh surface characteristics, plant composition (Vrieling et al., 2018), and the influence of non-photosynthetic matter on canopy structure, radiative transfer, and microclimate can lead to heterogeneity in phenological metrics from a point of remote sensors (Dronova and Taddeo, 2016). Additionally, unclear stressor-response relationships and uncertain interactions between multiple factors complicate ecosystem assessments (Chmura et al., 2019) and hinder causal inference regarding phenological variations (Dronova and Taddeo, 2022). While our study focuses on the influence of seasonal meteorological variations on saltmarsh vegetation phenology, the impact of extreme climate events remains unknown and warrants further investigation in future studies (Mo et al., 2015; Lian et al., 2020). In particular, weak and inconsistent correlations with meteorological variables in our findings complicate the assessment of interacting stressors such as salinity, inundation dynamics, and temperature, which vary across spatial and temporal scales. To disentangle these effects and identify causal mechanisms, controlled mesocosm experiments are essential. Such experiments can isolate specific climatic drivers and provide mechanistic insight into species-specific responses under changing environmental conditions. Furthermore, our case study overlooks the role of vegetation succession, with changes in plant composition also leading to observed phenology change of the vegetation, which could bias the apparent effects of meteorological changes on phenology. Meanwhile, remote sensing provides a robust approach to address the complexities and need of long-term time series of phenology and interpretation in dynamic ecosystems like saltmarshes, enabling more effective conservation strategies in a changing climate.

5. Conclusion

This study shows that saltmarsh vegetation phenology varies among plant species and communities, shaped by tidal emergence and diverse meteorological conditions. We present evidence of an advancing green-up and an extended growing season in some saltmarshes in response to

meteorological conditions. The growing season starts earlier for vegetation communities in higher intertidal areas compared to vegetation in lower elevated areas. Saltmarsh vegetation phenology is shaped by seasonal temperature and freshwater conditions with varying effects spatially. Furthermore, the phenological asynchrony was detected among four studied species. This study highlights the complex interactions between saltmarsh vegetation and meteorological conditions, providing valuable insights for predicting the resilience of saltmarsh ecosystem services and informing targeted conservation strategies at the regional estuarine scale.

Declaration of generative AI and AI-assisted technologies in the writing process

During the preparation of this work, the authors used GenAI tools, including ChatGPT and DeepSeek, in order to enhance language, grammar, and overall clarity. After using these tools/services, the authors reviewed and edited the content as needed and take full responsibility for the content of the publication.

CRediT authorship contribution statement

Jing Feng: Writing – review & editing, Writing – original draft, Visualization, Resources, Methodology, Investigation, Formal analysis, Data curation, Conceptualization. **Tim J. Grandjean:** Writing – review & editing, Visualization, Formal analysis, Conceptualization. **Xuerong Wu:** Writing – review & editing. **Johan van de Koppel:** Writing – review & editing, Supervision, Conceptualization. **Daphne van der Wal:** Writing – review & editing, Visualization, Supervision, Resources, Project administration, Methodology, Investigation, Conceptualization.

Declaration of competing interest

The authors declare that they have no known competing financial interests or personal relationships that could have appeared to influence the work reported in this paper.

Acknowledgements

We gratefully thank Annette Wielemaker for assistance with GIS data preprocessing, and our colleagues at the dept of Estuarine and Delta Systems (EDS) of NIOZ for suggestions on data analysis, visualization and manuscript writing. The first author (J. Feng) was supported by the China Scholarship Council, China (CSC, grant number: 202004910421).

Appendix A. Supplementary data

Supplementary data to this article can be found online at https://doi.org/10.1016/j.ecolind.2025.114219.

Data availability

The derived data and code can be found in the 4TU. Research Data repository with the link https://doi.org/10.4121/ae92386c-56be-4ff4-bc13-cc4f84a1486e. The raw data including open source maps of emersion duration, elevation, vegetation and ecotope are available from Rijkswaterstaat (https://rijkswaterstaatdata.nl/). Monthly meteorological data of station Vlissingen are available from Royal Netherlands Meteorological Institute (https://knmi.nl/). The time-series data of the drought index are available from the Global SPEI database, SPEIbase (https://spei.csic.es/database.html).

References

Antala, M., Juszczak, R., Van Der Tol, C., Rastogi, A., 2022. Impact of climate change-induced alterations in peatland vegetation phenology and composition on carbon balance. Sci. Total Environ. 827, 154294. https://doi.org/10.1016/j.scitotenv.2022.154294.

Antão, L.H., Bates, A.E., Blowes, S.A., Waldock, C., Supp, S.R., Magurran, A.E., Dornelas, M., Schipper, A.M., 2020. Temperature-related biodiversity change across temperate marine and terrestrial systems. Nat. Ecol. Evol. 4, 927–933. https://doi.org/10.1038/s41559-020-1185-7.

Baeyens, W., Van Eck, B., Lambert, C., Wollast, R., Goeyens, L., 1998. General description of the Scheldt estuary. Hydrobiologia 366, 1–14. https://doi.org/10.1023/A:1003164009031.

Bao, Y., Tian, H., Wang, X., 2024. Effects of climate change and ozone on vegetation phenology on the Tibetan Plateau. Sci. Total Environ. 932, 172780. https://doi.org/10.1016/j.scitotenv.2024.172780.

Beguería, S., Vicente-Serrano, S.M., Reig, F., Latorre, B., 2014. Standardized precipitation evapotranspiration index (SPEI) revisited: Parameter fitting, evapotranspiration models, tools, datasets and drought monitoring. Int. J. Climatol. 34, 3001–3023. https://doi.org/10.1002/joc.3887.

Berrached, R., Kadik, L., Ait Mouheb, H., Prinzing, A., 2017. Deep roots delay flowering and relax the impact of floral traits and associated pollinators in steppe plants. PLoS One 12, e0173921. https://doi.org/10.1371/journal.pone.0173921.

Buffington, K.J., Dugger, B.D., Thorne, K.M., 2018. Climate-related variation in plant peak biomass and growth phenology across Pacific Northwest tidal marshes. Estuar. Coast. Shelf Sci. 202, 212–221. https://doi.org/10.1016/j.ecss.2018.01.006.

Cardell, M.F., Amengual, A., Romero, R., Ramis, C., 2020. Future extremes of temperature and precipitation in Europe derived from a combination of dynamical and statistical approaches. Int. J. Climatol. 40, 4800–4827. https://doi.org/10.1002/joc.6490.

Chen, Y., Kirwan, M.L., 2022. Climate-driven decoupling of wetland and upland biomass trends on the mid-Atlantic coast. Nat. Geosci. 15, 913–918. https://doi.org/10.1038/s41561-022-01041-x.

Chmura, H.E., Kharouba, H.M., Ashander, J., Ehlman, S.M., Rivest, E.B., Yang, L.H., 2019. The mechanisms of phenology: The patterns and processes of phenological shifts. Ecol. Monogr. 89, e01337. https://doi.org/10.1002/ecm.1337.

Cleland, E.E., Chiariello, N.R., Loarie, S.R., Mooney, H.A., Field, C.B., 2006. Diverse responses of phenology to global changes in a grassland ecosystem. PNAS 103, 13740–13744. https://doi.org/10.1073/pnas.0600815103.

Cleland, E.E., Wolkovich, E.M., 2024. Effects of phenology on plant community assembly and structure. Annu. Rev. Ecol. Evol. Syst. 55, 471–492. https://doi.org/10.1146/annurev-ecolsys-102722-011653.

Davy, A.J., Bishop, G.F., Costa, C.S.B., 2001. Salicornia L.(Salicornia pusilla J. woods, S. ramosissima J. woods, S. europaea L., S. obscura PW ball & tutin, S. nitens PW ball & tutin, S. fragilis PW ball & tutin and S. dolichostachya moss). J. Ecol. 89, 681–707. https://doi.org/10.1046/j.0022-0477.2001.00607.x.

De Vriend, H.J., Wang, Z.B., Ysebaert, T., Herman, P.M.J., Ding, P., 2011. Eco-morphological problems in the Yangtze Estuary and the Western Scheldt. Wetlands 31, 1033–1042. https://doi.org/10.1007/s13157-011-0239-7.

Dieleman, W.I.J., Vicca, S., Dijkstra, F.A., Hagedorn, F., Hovenden, M.J., Larsen, K.S., Morgan, J.A., Volder, A., Beier, C., Dukes, J.S., King, J., 2012. Simple additive effects are rare: A quantitative review of plant biomass and soil process responses to combined manipulations of and temperature. Glob. Chang. Biol. 18, 2681–2693. https://doi.org/10.1111/j.1365-2486.2012.02745.x.

Dronova, I., Taddeo, S., 2016. Canopy leaf area index in non-forested marshes of the California delta. Wetlands 36, 705–716. https://doi.org/10.1007/s13157-016-0780-5.

Dronova, I., Taddeo, S., 2022. Remote sensing of phenology: Towards the comprehensive indicators of plant community dynamics from species to regional scales. J. Ecol. 110, 1460–1484. https://doi.org/10.1111/1365-2745.13897.

Dronova, I., Taddeo, S., Harris, K., 2022. Plant diversity reduces satellite-observed phenological variability in wetlands at a national scale. Sci. Adv. 8, eabl8214. https://doi.org/10.1126/sciadv.abl8214.

Eilers, P.H.C., 2003. A perfect smoother. Anal. Chem. 75, 3631–3636. https://doi.org/10.1021/ac034173t.

Eller, F., Skálová, H., Caplan, J.S., Bhattarai, G.P., Burger, M.K., Cronin, J.T., Caplan, J. S., Bhattarai, G.P., Burger, M.K., Cronin, J.T., Guo, W.Y., Guo, X., Hazelton, E.L., Kettenring, K.M., Lambertini, C., 2017. Cosmopolitan species as models for ecophysiological responses to global change: the common reed Phragmites australis. Front. Plant Sci. 8, 1833. https://doi.org/10.3389/fpls.2017.01833.

ESRI. 2023. ArcGIS Pro: release 3.2.2. Redlands, CA:Environmental Systems Research Institute.

Feng, J., Grandjean, T.J., Van de Koppel, J., Van der Wal, D., 2025. A spatiotemporal framework to assess the bio-geomorphic interplay of saltmarsh vegetation and tidal emergence (Western Scheldt estuary). Int. J. Appl. Earth Obs. Geoinf. 136, 104337. https://doi.org/10.1016/j.jag.2024.104337.

Filippa, G., Cremonese, E., Migliavacca, M., Galvagno, M., Forkel, M., Wingate, L., Tomelleri, E., Di Cella, U.M., Richardson, A.D., 2016. Phenopix: A R package for image-based vegetation phenology. Agric. For. Meteorol. 220, 141–150. https://doi.org/10.1016/j.agrformet.2016.01.006.

Fivash, G.S., Temmerman, S., Kleinhans, M.G., Heuner, M., Van der Heide, T., Bouma, T. J., 2023. Early indicators of tidal ecosystem shifts in estuaries. Nat. Commun. 14, 1911. https://doi.org/10.1038/s41467-023-37444-6.

Flowers, T.J., Colmer, T.D., 2015. Plant salt tolerance: Adaptations in halophytes. Ann. Bot. 115, 327–331. https://doi.org/10.1093/aob/mcu267.

Forster, P.M., Smith, C., Walsh, T., Lamb, W.F., Lamboll, R., Hall, B., Hauser, M., Ribes, A., Rosen, D., Gillett, N.P., Palmer, M.D., 2024. Indicators of Global climate change 2023: Annual update of key indicators of the state of the climate system and human influence. Earth Syst. Sci. Data 16, 2625–2658. https://doi.org/10.5194/essd-16-2625-2024.

Fu, Y., Li, X., Zhou, X., Geng, X., Guo, Y., Zhang, Y., 2020. Progress in plant phenology modeling under global climate change. Sci. China Earth Sci. 63, 1237–1247. https://doi.org/10.1007/s11430-019-9622-2.

Fu, Y.H., Piao, S., Zhao, H., Jeong, S.J., Wang, X., Vitasse, Y., Ciais, P., Janssens, I.A., 2014. Unexpected role of winter precipitation in determining heat requirement for spring vegetation green-up at northern middle and high latitudes. Glob. Chang. Biol. 20, 3743–3755. https://doi.org/10.1111/gcb.12610.

Gallego-Tévar, B., Grewell, B.J., Futrell, C.J., Drenovsky, R.E., Castillo, J.M., 2019. Interactive effects of salinity and inundation on native Spartina foliosa, invasive S. densiflora and their hybrid from San Francisco Estuary California. Ann. Bot. 125, 377–389. https://doi.org/10.1093/aob/mcz170.

Gorelick, N., Hancher, M., Dixon, M., Ilyushchenko, S., Thau, D., Moore, R., 2017. Google Earth Engine: Planetary-scale geospatial analysis for everyone. Remote Sens. Environ. 202, 18–27. https://doi.org/10.1016/j.rse.2017.06.031.

Grime, J.P., 1977. Evidence for the existence of three primary strategies in plants and its relevance to ecological and evolutionary theory. Am. Nat. 111, 1169–1194. https://doi.org/10.1086/283244.

Harper, W.V., 2016. Reduced Major Axis Regression. In N. Balakrishnan, T. Colton, B. Everitt, W. Piegorsch, F. Ruggeri, & J. L. Teugels (Eds.), Wiley StatsRef: Statistics Reference Online (1st ed.). Wiley, New Jersey, pp. 1–6. https://doi.org/10.1002/9781118445112.stat07912.

Hroudová, Z., Zákravský, P., Flegrová, M., 2014. The tolerance to salinity and nutrient supply in four European Bolboschoenus species (B. maritimus, B. laticarpus, B. planiculmis and B. yagara) affects their vulnerability or expansiveness. Aquat. Bot. 112, 66–75. https://doi.org/10.1016/j.aquabot.2013.07.012.

Jeong, S.J., Gim, C.H., Brown, H.J., 2011. Phenology shifts at start vs. end of growing season in temperate vegetation over the Northern Hemisphere for the period 1982–2008. Glob. Chang. Biol. 17, 2385–2399. https://doi.org/10.1111/j.1365-2486.2011.02397.x.

Jiang, N., Shen, M., Chen, J., Yang, W., Zhu, X., Wang, X., Peñuelas, J., 2023. Continuous advance in the onset of vegetation green-up in the Northern Hemisphere, during hiatuses in spring warming. npj Clim. Atmos. Sci. 6, 7. https://doi.org/10.1038/s41612-023-00343-0.

Jiang, Z., Huete, A.R., Didan, K., Miura, T., 2008. Development of a two-band enhanced vegetation index without a blue band. Remote Sens. Environ. 112, 3833–3845. https://doi.org/10.1016/j.rse.2008.06.006.

Kers, A.S., Walburg, L., Bakker, J., Daane, A.H., de Jong, D.J., Schrijver, M., Lievense, P., Dekker, L., de Klerk, J., 2013. Dienstbeschrijving Zoute ecotopenkaarten. Rijkswaterstaat CIV / Zee & Delta, Delft / Middelburg.

Knight, C.A., Ackerly, D.D., 2003. Evolution and plasticity of photosynthetic thermal tolerance, specific leaf area and leaf size: Congeneric species from desert and coastal environments. New Phytol. 160, 337–347. https://doi.org/10.1046/j.1469-8137.2003.00880.x.

Kong, D., Zhang, Y., Wang, D., Chen, J., Gu, X., 2020. Photoperiod explains the asynchronization between vegetation carbon phenology and vegetation greenness phenology. J. Geophys. Res.:biogeosci. 125, e2020JG005636. https://doi.org/10.1029/2020JG005636.

Kong, D., McVicar, T.R., Xiao, M., Zhang, Y., Peña-Arancibia, J.L., Filippa, G., Xie, Y., Gu, X., 2022. phenofit: An R package for extracting vegetation phenology from time series remote sensing. Methods Ecol. Evol. 13, 1508–1527. https://doi.org/10.1111/2041-210X.13870.

Kong, D., Zhang, Y., Gu, X., Wang, D., 2019. A robust method for reconstructing global MODIS EVI time series on the Google Earth Engine. ISPRS J. Photogramm. Remote Sens. 155, 13–24. https://doi.org/10.1016/j.isprsjprs.2019.06.014.

Koppejan, H., 2000. Toelichting bij de vegetatiekartering Westerschelde 1998: op basis van false colour-luchtfoto's 1:5000/10000. Rijkswaterstaat, Meetkundige Dienst, afdeling GAE, Delft.

Kromkamp, J.C., Van Engeland, T., 2010. Changes in phytoplankton biomass in the western scheldt estuary during the period 1978–2006. Estuaries Coast 33, 270–285. https://doi.org/10.1007/s12237-009-9215-3.

Laengner, M.L., Siteur, K., Van der Wal, D., 2019. Trends in the seaward extent of saltmarshes across europe from long-term satellite data. Remote Sens. 11, 1653. https://doi.org/10.3390/rs11141653.

Laengner, M.L., Van der Wal, D., 2022. Satellite-derived trends in inundation frequency reveal the fate of saltmarshes. Front. Mar. Sci. 9, 942719. https://doi.org/10.3389/fmars.2022.942719.

Lee, J.-Y., Marotzke, J., Bala, G., Cao, L., Corti, S., Dunne, J.P., Engelbrecht, F., Fischer, E., Fyfe, J.C., Jones, C., Maycock, A., Mutemi, J., Ndiaye, O., Panickal, S., Zhou, T., 2021. Future global climate: scenario-based projections and near-term information. In: Climate Change 2021: The Physical Science Basis. Contribution of Working Group I to the Sixth Assessment Report of the Intergovernmental Panel on Climate Change. Cambridge University Press, Cambridge, United Kingdom and New York, NY, USA, pp. 553–672.

Legendre, P., 2000. Comparison of permutation methods for the partial correlation and partial mantel tests. J. Stat. Comput. Simul. 67, 37–73. https://doi.org/10.1080/00949650008812035.

Lian, X., Piao, S., Li, L.Z., Li, Y., Huntingford, C., Ciais, P., Cescatti, A., Janssens, I.A., Peñuelas, J., Buermann, W., Chen, A., 2020. Summer soil drying exacerbated by earlier spring greening of northern vegetation. Sci. Adv. 6, eaax0255. https://doi.org/10.1126/sciadv.aax0255.

Mann, H.B., 1945. Nonparametric tests against trend. Econometrica 13, 245–259. https://doi.org/10.2307/1907187.

Meire, P., Ysebaert, T., Damme, S.V., Bergh, E.V.D., Maris, T., Struyf, E., 2005. The Scheldt estuary: A description of a changing ecosystem. Hydrobiologia 540, 1–11. https://doi.org/10.1007/s10750-005-0896-8.

Meng, F., Felton, A.J., Mao, J., Cong, N., Smith, W.K., Körner, C., Hu, Z., Hong, S., Knott, J., Yan, Y., Guo, B., 2024. Consistent time allocation fraction to vegetation green-up versus senescence across northern ecosystems despite recent climate change. Sci. Adv. 10, eadn2487. https://doi.org/10.1126/sciadv.adn2487.

Meng, F., Liu, D., Wang, Y., Wang, S., Wang, T., 2023. Negative relationship between photosynthesis and late-stage canopy development and senescence over Tibetan Plateau. Glob. Chang. Biol. 29, 3147–3158. https://doi.org/10.1111/gcb.16668.

Miller, G.J., Dronova, I., Oikawa, P.Y., Knox, S.H., Windham-Myers, L., Shahan, J., Stuart-Haëntjens, E., 2021. The potential of satellite remote sensing time series to uncover wetland phenology under unique challenges of tidal setting. Remote Sens. 13, 3589. https://doi.org/10.3390/rs13183589.

Mo, Y., Kearney, M.S., Turner, R.E., 2019. Feedback of coastal marshes to climate change: Long-term phenological shifts. Ecol. Evol. 9, 6785–6797. https://doi.org/10.1002/ece3.5215.

Mo, Y., Michael, K., Bahram, M., 2017. Drought-associated phenological changes of coastal marshes in Louisiana. Ecosphere 8, e01811. https://doi.org/10.1002/ecs2.1811.

Mo, Y., Momen, B., Kearney, M.S., 2015. Quantifying moderate resolution remote sensing phenology of Louisiana coastal marshes. Ecol. Model. 312, 191–199. https://doi.org/10.1016/j.ecolmodel.2015.05.022.

Mo, Y., Chen, S., Wu, Z., Tang, J., Fu, Y., 2024. The advancement in spring vegetation phenology in the northern hemisphere will reverse after 2060 under future moderate warming scenarios. Earth's Future 12, e2023EF003788. https://doi.org/10.1029/2023EF003788.

Moffett, K.B., Robinson, D.A., Gorelick, S.M., 2010. Relationship of salt marsh vegetation zonation to spatial patterns in soil moisture, salinity, and topography. Ecosystems 13, 1287–1302. https://doi.org/10.1007/s10021-010-9385-7.

Morellato, L.P.C., Alberton, B., Alvarado, S.T., Borges, B., Buisson, E., Camargo, M.G.G., Cancian, L.F., Carstensen, D.W., Escobar, D.F., Leite, P.T., Mendoza, I., 2016. Linking plant phenology to conservation biology. Biol. Conserv. 195, 60–72. https://doi.org/10.1016/j.biocon.2015.12.033.

Noyce, G.L., Smith, A.J., Kirwan, M.L., Rich, R.L., Megonigal, J.P., 2023. Oxygen priming induced by elevated CO2 reduces carbon accumulation and methane emissions in coastal wetlands. Nat. Geosci. 16, 63–68. https://doi.org/10.1038/s41561-022-01070-6.

O'Donnell, J., Schalles, J., 2016. Examination of abiotic drivers and their influence on spartina alterniflora biomass over a twenty-eight year period using landsat 5 TM satellite imagery of the Central Georgia Coast. Remote Sens. 8, 477. https://doi.org/10.3390/rs8060477.

Packer, J.G., Meyerson, L.A., Skálová, H., Pyšek, P., Kueffer, C., 2017. Biological flora of the British Isles: Phragmites australis. J. Ecol. 105, 1123–1162. https://doi.org/10.1111/1365-2745.12797.

Park, T., Chen, C., Macias-Fauria, M., Tømmervik, H., Choi, S., Winkler, A., Bhatt, U.S., Walker, D.A., Piao, S., Brovkin, V., Nemani, R.R., 2019. Changes in timing of seasonal peak photosynthetic activity in northern ecosystems. Glob. Chang. Biol. 25, 2382–2395. https://doi.org/10.1111/gcb.14638.

Peichl, M., Gažovič, M., Vermeij, I., De Goede, E., Sonnentag, O., Limpens, J., Nilsson, M. B., 2018. Peatland vegetation composition and phenology drive the seasonal trajectory of maximum gross primary production. Sci. Rep. 8, 8012. https://doi.org/10.1038/s41598-018-26147-4.

Pérez-Harguindeguy, N., Díaz, S., Garnier, E., Lavorel, S., Poorter, H., Bret-Harte, M.S., Cornwell, W.K., Craine, J.M., Gurvich, D.E., Urcelay, C., Veneklaas, E.J., Reich, P.B., Poorter, L., Jaureguiberry, P., Wright, I.J., Ray, P., Enrico, L., Pausas, J.G., De Vos, A. C., Buchmann, N., Funes, G., Quetier, F., Hodgson, J.G., Morgan, H.D., Ter Steege, H., Van der Heijden, M.G.A., Sack, L., Blonder, B., Poschlod, P., Vaieretti, M. V., Conti, G., Staver, A.C., Aquino, S., Cornelissen, J.H.C., 2013. New handbook for standardised measurement of plant functional traits worldwide. Aust. J. Bot. 61, 167–234. https://doi.org/10.1071/BT12225.

Piao, S., Liu, Q., Chen, A., Janssens, I.A., Fu, Y., Dai, J., Liu, L., Lian, X.U., Shen, M., Zhu, X., 2019a. Plant phenology and global climate change: Current progresses and challenges. Glob. Chang. Biol. 25, 1922–1940. https://doi.org/10.1111/gcb.14619.

Piao, S., Tan, J., Chen, A., Fu, Y.H., Ciais, P., Liu, Q., Janssens, I.A., Vicca, S., Zeng, Z., Jeong, S.J., Li, Y., 2015. Leaf onset in the northern hemisphere triggered by daytime temperature. Nat. Commun. 6, 6911. https://doi.org/10.1038/ncomms7911.

Piao, S., Wang, X., Park, T., Chen, C., Lian, X.U., He, Y., Bjerke, J.W., Chen, A., Ciais, P., Tømmervik, H., Nemani, R.R., Myneni, R.B., 2019b. Characteristics, drivers and feedbacks of global greening. Nat. Rev. Earth Environ. 1, 14–27. https://doi.org/10.1038/s43017-019-0001-x.

Pranger, D.P., Tolman, M.E., 2012. Toelichting bij de vegetiekartering Westerschelde 2010: op basis van false colour-luchtfoto's 1:5000. Rijkswaterstaat-DID, Delft.

R Core Team, 2023. R: A language and environment for statistical computing. R Foundation for Statistical Computing, Vienna, Austria http://www.R-project.org.

Reitsma, J.M., 2006. Toelichting bij de vegetatiekartering Westerschelde 2004: op basis van false colour-luchtfoto's 1:5000/1:1000. Rijkswaterstaat-AGI, Delft.

Reitsma, J.M., de Jong, J., 2018. Toelichting bij de Vegetatiekartering Westerschelde 2016: op basis van false colour-luchtfoto's 1:5.000. Rijkswaterstaat-CIV, Servicedesk Geo-informatie: Delft.

Ren, P., Li, P., Zhou, X., Liu, Z., Tang, J., Zhang, C., Zou, Z., Li, T., Peng, C., 2024. Shifts in plant phenology significantly affect the carbon allocation in different plant organs. Ecol. Lett. 27, e70024. https://doi.org/10.1111/ele.70024.

Renner, S.S., Zohner, C.M., 2018. Climate change and phenological mismatch in trophic interactions among plants, insects, and vertebrates. Annu. Rev. Ecol. Evol. Syst. 49, 165–182. https://doi.org/10.1146/annurev-ecolsys-110617-062535.

Richardson, A.D., Keenan, T.F., Migliavacca, M., Ryu, Y., Sonnentag, O., Toomey, M., 2013. Climate change, phenology, and phenological control of vegetation feedbacks

to the climate system. Agric. For. Meteorol. 169, 156–173. https://doi.org/10.1016/j.agrformet.2012.09.012.
Rijkswaterstaat, 2016. Getijtafels voor Nederland (in Dutch). Sdu, the Hague, 160 pp.
Robinson, A., Lehmann, J., Barriopedro, D., Rahmstorf, S., Coumou, D., 2021. Increasing heat and rainfall extremes now far outside the historical climate. npj Clim. Atmos. Sci. 4, 45. https://doi.org/10.1038/s41612-021-00202-w.
Sen, P.K., 1968. Estimates of the regression coefficient based on Kendall's Tau. J. Am. Stat. Assoc. 63, 1379–1389. https://doi.org/10.1080/01621459.1968.10480934.
Shen, X., Liu, B., Xue, Z., Jiang, M., Lu, X., Zhang, Q., 2019. Spatiotemporal variation in vegetation spring phenology and its response to climate change in freshwater marshes of Northeast China. Sci. Total Environ. 666, 1169–1177. https://doi.org/10.1016/j.scitotenv.2019.02.265.
Stevens, M.H.H., Carson, W.P., 2001. Phenological complementarity, species diversity, and ecosystem function. Oikos 92, 291–296. https://doi.org/10.1034/j.1600-0706.2001.920211.x.
Suggitt, A.J., Wilson, R.J., Isaac, N.J.B., Beale, C.M., Auffret, A.G., August, T., Bennie, J. J., Crick, H.Q.P., Duffield, S., Fox, R., Hopkins, J.J., Macgregor, N.A., Morecroft, M. D., Walker, K.J., Maclean, I.M.D., 2018. Extinction risk from climate change is reduced by microclimatic buffering. Nat. Clim. Change 8, 713–717. https://doi.org/10.1038/s41558-018-0231-9.
Sun, C., Li, J., Liu, Y., Zhao, S., Zheng, J., Zhang, S., 2023. Tracking annual changes in the distribution and composition of saltmarsh vegetation on the Jiangsu coast of China using Landsat time series–based phenological parameters. Remote Sens. Environ. 284, 113370. https://doi.org/10.1016/j.rse.2022.113370.
Tavora, J., Salama, M.S., Penning de Vries, M., Mannaerts, C.M., Van der Wal, D., 2023. Detecting the effects of extreme events on estuarine suspended particulate matter using satellite remote sensing (Scheldt Estuary): Challenges and opportunities. Remote Sens. 15, 670. https://doi.org/10.3390/rs15030670.
Temmerman, S., Horstman, E.M., Krauss, K.W., Mullarney, J.C., Pelckmans, I., Schoutens, K., 2023. Marshes and mangroves as nature-based coastal storm buffers. Ann. Rev. Mar. Sci. 15, 95–118. https://doi.org/10.1146/annurev-marine-040422-092951.
Van de Koppel, J., Van der Wal, D., Bakker, J.P., Herman, P.M.J., 2005. Self-organization and vegetation collapse in salt marsh ecosystems. Am. Nat. 165, E1–E12. https://doi.org/10.1086/426602.
Van der Wal, D., Wielemaker-Van den Dool, A., Herman, P.M.J., 2008. Spatial patterns, rates and mechanisms of saltmarsh cycles (Westerschelde, the Netherlands). Estuar. Coast. Shelf Sci. 76, 357–368. https://doi.org/10.1016/j.ecss.2007.07.017.
Vautard, R., Cattiaux, J., Happé, T., Singh, J., Bonnet, R., Cassou, C., Coumou, D., D'andrea, F., Faranda, D., Fischer, E., Ribes, A., 2023. Heat extremes in Western Europe increasing faster than simulated due to atmospheric circulation trends. Nat. Commun. 14, 6803. https://doi.org/10.1038/s41467-023-42143-3.
Vicente-Serrano, S.M., Beguería, S., López-Moreno, J.I., 2010. A multiscalar drought index sensitive to global warming: The standardized precipitation evapotranspiration index. J. Clim. 23, 1696–1718. https://doi.org/10.1175/2009JCLI2909.1.
Von Asmuth, J.R., Stenfert-Steehouwer, E.R., Reitsma, J.M., 1996. De schorren van de Westerschelde 1990/1993. Rijkswaterstaat, Meetkundige Dienst, afdeling. GAE, Delft.
Vrieling, A., Meroni, M., Darvishzadeh, R., Skidmore, A.K., Wang, T., Zurita-Milla, R., Oosterbeek, K., O'Connor, B., Paganini, M., 2018. Vegetation phenology from Sentinel-2 and field cameras for a Dutch barrier island. Remote Sens. Environ. 215, 517–529. https://doi.org/10.1016/j.rse.2018.03.014.
Wang, H., Dai, J., Peñuelas, J., Ge, Q., Fu, Y.H., Wu, C., 2022. Winter warming offsets one half of the spring warming effects on leaf unfolding. Glob. Chang. Biol. 28, 6033–6049. https://doi.org/10.1111/gcb.16358.
Wang, Q., Luo, M., Cui, B., Chen, C., Xie, T., Li, X., Lu, F., 2024. Effects of varied inundation characteristics on early life stages of a salt marsh plant. Front. Mar. Sci. 11, 1449034. https://doi.org/10.3389/fmars.2024.1449034.
Wu, D., Zhao, X., Liang, S., Zhou, T., Huang, K., Tang, B., Zhao, W., 2015. Time-lag effects of global vegetation responses to climate change. Glob. Chang. Biol. 21, 3520–3531. https://doi.org/10.1111/gcb.12945.
Xu, Y., Li, M., Liu, Z., Gong, Y., Wu, Z., Pu, X., Fu, Y.H., 2024. From delay to advance: the impact of increasing drought on autumn photosynthetic phenology in subtropical and tropical forests. Geophys. Res. Lett. 51, e2024GL112054. https://doi.org/10.1029/2024GL112054.
Yando, E.S., Jones, S.F., James, W.R., Colombano, D.D., Montemayor, D.I., Nolte, S., Raw, J.L., Ziegler, S.L., Chen, L., Daffonchio, D., Fusi, M., Rogers, K., Sergienko, L., 2023. An integrative salt marsh conceptual framework for global comparisons. Limnol. Oceanogr. Lett. 8, 830–849. https://doi.org/10.1002/lol2.10346.
Zeng, K., Sentinella, A.T., Armitage, C., Moles, A.T., 2024. Species that require long-day conditions to flower are not advancing their flowering phenology as fast as species without photoperiod requirements. Ann. Bot. 135, 113–124. https://doi.org/10.1093/aob/mcae121.
Zhang, Q., Kong, D., Shi, P., Singh, V.P., Sun, P., 2018. Vegetation phenology on the Qinghai-Tibetan Plateau and its response to climate change (1982–2013). Agric. For. Meteorol. 248, 408–417. https://doi.org/10.1016/j.agrformet.2017.10.026.
Zhang, Z., Luo, X., Friess, D.A., Wang, S., Li, Y., Li, Y., 2024. Stronger increases but greater variability in global mangrove productivity compared to that of adjacent terrestrial forests. Nat. Ecol. Evol. https://doi.org/10.1038/s41559-023-02264-w.
Zhao, Z., Zhang, L., Yuan, L., Bouma, T.J., 2023. Pinpointing stage-specific causes of recruitment bottlenecks to optimize seed-based wetland restoration. J. Appl. Ecol. 60, 330–341. https://doi.org/10.1111/1365-2664.14325.
Zhu, X., Meng, L., Zhang, Y., Weng, Q., Morris, J., 2019. Tidal and meteorological influences on the growth of invasive Spartina alterniflora: evidence from UAV remote sensing. Remote Sens. 11, 1208. https://doi.org/10.3390/rs11101208.
Zou, Y.A., Tang, C.D., Niu, J.Y., Wang, T.H., Xie, Y.H., Guo, H., 2016. Migratory waterbirds response to coastal habitat changes: Conservation implications from long-term detection in the Chongming Dongtan Wetlands China. Estuaries Coast 39, 273–286. https://doi.org/10.1007/s12237-015-9991-x.